Semicond. Sci. Technol. **24** (2009) 055005 (5pp) doi:10.1088/0268-1242/24/5/055005

Study of the leakage current mechanism in Schottky contacts to $Al_{0.25}Ga_{0.75}N/GaN$ heterostructures with AlN interlayers

Sen Huang, Bo Shen, Fu-Jun Xu, Fang Lin, Zhen-Lin Miao, Jie Song, Lin Lu, Long-Bin Cen, Li-Wen Sang, Zhi-Xin Qin, Zhi-Jian Yang and Guo-Yi Zhang

State Key Laboratory of Artificial Microstructure and Mesoscopic Physics, School of Physics, Peking University, Beijing 100871, People's Republic of China

E-mail: bshen@pku.edu.cn

Received 11 February 2009, in final form 11 March 2009
Published 3 April 2009
Online at stacks.iop.org/SST/24/055005

Abstract

The leakage current mechanism in Schottky contacts (SCs) to $Al_{0.25}Ga_{0.75}N/GaN$ heterostructures incorporated by a thin high-temperature (HT) AlN interlayer has been investigated using current–voltage measurements, atomic force microscopy and deep level transient spectroscopy. It is found that the HT AlN interlayer thickness has a significant effect on the leakage current in SCs. The leakage current density decreases to 1.1×10^{-4} A cm^{-2} when the growth time of the AlN interlayer increases from 0 to 10 s, and then changes to increase with increasing growth time. Correspondingly, the heterostructure with the AlN growth time of 10 s has the least number of surface pinholes. The thickness of the HT AlN also influences the density of electron traps with the activation energy of 0.762 eV in an $Al_{0.25}Ga_{0.75}N$ barrier. It is suggested that the HT AlN interlayer adjusts the microstructure and the defect state density in the $Al_{1-x}Ga_xN$ barrier, and the leakage via these defect states makes the main contribution to the leakage current in SCs to $Al_{1-x}Ga_xN/GaN$ heterostructures.

1. Introduction

GaN-based high electron mobility transistors (HEMTs) are excellent candidates for high-temperature, high-voltage and high-power operation at microwave as well as lower frequencies [1, 2]. Maximizing the product of the two-dimensional electron gas (2DEG) mobility μ and the 2DEG sheet density n has a direct impact on the output power density of the device, while minimizing the off-state leakage current in HEMTs is essential for their incorporation into circuits and systems in which low noise and low power consumption demand [3]. Hsu and Walukiewicz suggested that inserting a very thin AlN layer between $Al_{1-x}Ga_xN$ and GaN would significantly improve the 2DEG mobility and slightly enhance the 2DEG concentration, which resulted in a much improved output power density of HEMTs [4]. We think a proper AlN interlayer will not merely increase the 2DEG mobility, but also reduce the leakage current in Schottky contacts (SCs) to $Al_{1-x}Ga_xN/GaN$ heterostructures by improving the film quality of the $Al_{1-x}Ga_xN$ barrier [5].

However, little attention has been paid to the effect of the AlN interlayer on the leakage current in SCs to $Al_{1-x}Ga_xN/GaN$ heterostructures. Recently, it has been suggested that the traps in the $Al_{1-x}Ga_xN$ barrier play an important role in changing the leakage current in SCs to $Al_{1-x}Ga_xN/GaN$ heterostructures [2, 6]. In this study, the influence of high-temperature (HT) AlN interlayer on the reverse-biased leakage current in Ni/Au SCs to $Al_{0.25}Ga_{0.75}N/GaN$ heterostructures as well as the deep level traps in the $Al_{0.25}Ga_{0.75}N$ barrier have been investigated. The leakage through the traps in the $Al_{0.25}Ga_{0.75}N$ barrier is suggested to be the main leakage current mechanism in SCs to $Al_{0.25}Ga_{0.75}N/GaN$ heterostructures.

2. Experiments

$Al_{0.25}Ga_{0.75}N$/GaN heterostructures with a thin HT AlN interlayer were grown by metal-organic chemical vapor deposition (MOCVD) on the (0 0 0 1) surface of sapphire substrate. A nucleation GaN buffer layer was grown at 530 °C, followed by a 2.2 μm thick unintentionally doped GaN (i-GaN) layer deposited at 1070 °C. Then, the temperature was increased to 1090 °C to grow a thin HT AlN interlayer to reduce the alloy disorder scattering and the 25 nm thick unintentionally doped $Al_{0.25}Ga_{0.75}N$ barrier. Six samples were prepared. The first one, named as S1, is a i-GaN epilayer without the HT AlN interlayer and $Al_{0.25}Ga_{0.75}N$ barrier. For other fives named as S2–S6, respectively, only the growth time of the HT AlN interlayer was changed, which means the different thickness of the HT AlN interlayer in these samples. The S2–S6 samples stand for the growth times of 0, 5 s, 10 s, 13 s and 16 s, respectively. According to the high-resolution transmission electron microscopy (HR-TEM) image of S5, the approximate thickness of the HT AlN interlayer with the growth time of 13 s is about 1 nm. Van der Paul geometry was adopted for Hall measurements. The room temperature mobility and the concentration of electrons in i-GaN are 408 $cm^2\ Vs^{-1}$ and $1.44 \times 10^{16}\ cm^{-3}$, respectively. The room temperature mobilities of the 2DEG from samples S2 to S6 are 893, 994, 1357, 1288 and 1255 $cm^2\ Vs^{-1}$, respectively.

Then, for the fabrication of Schottky diodes, ring-shaped Ohmic contacts were formed by standard photolithography on a sample surface, using a Ti/Al/Ni/Au (25/120/45/50 nm) alloy annealed at 850 °C in N_2 for 30 s in a rapid thermal annealing system. Conventional organic cleaning of sample surface was conducted before Schottky metallization. Circular SCs of Ni/Au (50/100 nm) with a diameter of 400 μm were deposited in the center of the Ohmic rings by e-beam evaporation. The separation between the Ohmic and SCs is 100 μm.

A high-resolution deep level transient spectroscopy (DLTS) spectrometer with a 100 mV, 2 MHz test signal, an Agilent 4155 C semiconductor parameter analyzer, and an Agilent 4294 A precision impedance analyzer with a 100 mV, 10 kHz test signal were used for DLTS, current–voltage (*I–V*) and capacitance–voltage (*C–V*) measurements, respectively. The usual trap parameters (the activation energy and the apparent capture cross section) were determined from an Arrhenius analysis of the DLTS peak position as a function of the rate window (e_n), typically varied between 4.4 and 220 s^{-1}. Surface morphology of $Al_{0.25}Ga_{0.75}N$/GaN heterostructures was probed using a contact-mode atomic force microscopy (AFM).

3. Results and discussion

Figure 1 shows the reverse-biased leakage current density at −8 V of the five Schottky barrier diodes (SBDs) on $Al_{0.25}Ga_{0.75}N$/GaN heterostructures with different thickness of the HT AlN interlayer. In order to minimize the wafer's nonuniformity, each value has been taken by averaging of more than ten good units on the same wafer. The inset shows

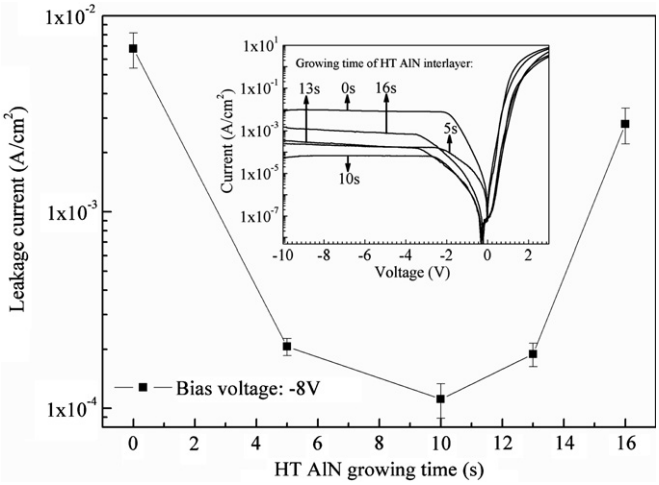

Figure 1. Leakage current density at −8 V of Au/Ni Schottky contacts to $Al_{0.25}Ga_{0.75}N$/GaN heterostructures with the growth time of the HT AlN interlayer of 0, 5 s, 10 s, 13 s and 16 s, respectively. The inset shows typical *I–V* curves from −10 V to 3 V for each sample.

five typical *I–V* curves from −10 to 3 V for each sample. The drifting of the minimum junction leakage current for S4, S5 and S6 to the minus direction is probably due to the charging of near-surface traps in the $Al_{0.25}Ga_{0.75}N$ barrier when increasing the applied voltage [7]. Calculation confirms that the trap-charging current is negligible compared with the leakage current at −8 V, so it will not affect the following discussion about the effect of the AlN interlayer thickness on the leakage current at below the pinch-off voltage. The fact that samples S4, S5 and S6 show much less forward current than those of S2 and S3 is probably caused by the increase of AlN thickness, which enhances the effective barrier height at the $Al_{0.25}Ga_{0.75}N$/GaN heterointerface [8]. The sample without the HT AlN interlayer (S2) shows the largest leakage current throughout the entire reverse-bias range. When the growth time of the AlN interlayer increases to 10 s (S4), the leakage current density decreases to $1.1 \times 10^{-4}\ A\ cm^{-2}$. However, the leakage current density changes to increase with increasing growth time after it exceeds 10 s.

According to the changing tendency of the leakage current, samples S2, S4 and S6 were chosen for AFM measurements. Figure 2(*a*) shows the surface morphology of S2 (without the AlN interlayer). A large number of pinholes spread all over it. Geng *et al* suggested that pinholes came from the extended coreless dislocations, which were originating in the GaN buffer layer [9]. However, much less pinholes appear on the surface of S4 (with 10 s AlN interlayer), as shown in figure 2(*b*). Moreover, clear terraces emerging from the surface of S4 indicate that S4 has better film quality than S2. When the growth time of the HT AlN interlayer increases to 16 s (S6), the surface morphology deteriorates again, as shown in figure 2(*c*), although the size and number of pinholes become smaller than those in S2.

Therefore, an appropriate thickness of the HT AlN interlayer can effectively reduce the surface pinholes and

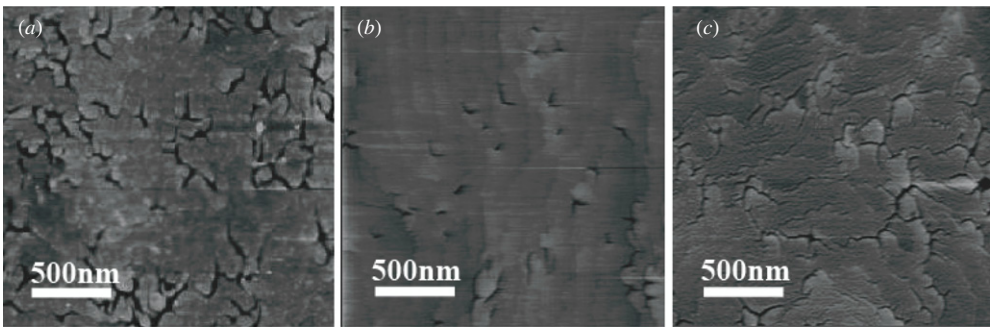

Figure 2. Representative 2 μm $\times$ 2 μm AFM images of samples (*a*) S2, (*b*) S4 and (*c*) S6.

clusters of pinholes in the $Al_{0.25}Ga_{0.75}N$ barrier. The thin HT AlN interlayer may have two effects. One is that it can alleviate the tensile strain in the $Al_{0.25}Ga_{0.75}N$ barrier layer [10]. The other is that it can terminate some of the threading dislocations (TDs) extended from the i-GaN layer. Both effects may reduce the number of surface pinholes in $Al_{0.25}Ga_{0.75}N$ films. However, as the growth time of the HT AlN prolongs, the strain in the HT AlN interlayer will grow up due to the large lattice mismatch between AlN and GaN, and new defects can also generate in the AlN interlayer [11].

Numerical calculation has been performed to investigate the leakage mechanism in SCs to $Al_{0.25}Ga_{0.75}N$/GaN heterostructures. Here, the total reverse-biased leakage current is described as follows:

$$I_{\mathrm{TL}} = I_{\mathrm{TE}} + I_{\mathrm{DT}} + I_{\mathrm{TFE}} + I_P + I_{\mathrm{TD}}, \tag{1}$$

where I_{TL} is the total leakage current, I_{TE} the thermionic emission current, I_{DT} the direct tunneling current, I_{TFE} the thermal field emission current, I_P the leakage through the pinholes and clusters of pinholes, I_{TD} the leakage through TDs with a screw component [12]. I_{TE}, I_{DT} and I_{TFE} can be written as follows [2]:

$$I_{\mathrm{TE}} = \mathrm{SA}^* T^2 \exp\left(-\frac{\phi_B}{kT}\right), \tag{2}$$

$$I_{\mathrm{DT}} = \frac{q^2 \mathrm{SE}^2}{8\pi h \phi_B} \exp\left(-\frac{\alpha}{E}\phi_B^{3/2}\right), \qquad E = \frac{V_G + \phi_B - \Delta\phi_C - \phi_{fb}}{d}. \tag{3}$$

$$I_{\mathrm{TFE}} = \frac{q\mathrm{SA}^* T}{k} \int_0^{\phi_B} f_{\mathrm{FD}} P \, d\phi, \qquad P = \exp\left(-\frac{\alpha}{E}\phi^{3/2}\right). \tag{4}$$

All symbols in the above equations take the same meaning as those in [2] except that the barrier doping is ignored. Considering ϕ_B lowering due to image force and band gap reduction with temperature, we simulate I_{TE}, I_{DT} and I_{TFE} with initial assumption of $\phi_{B0} = 1.4$ V, $\Delta\phi_C = 0.34$ V [13], $m = 0.17m_0$ [2], $d = 25$ nm and $\phi_{fb} = 0.075$ V (the activation energy is calculated from temperature-dependant Hall measurements of S1).

The current density, which is obtained by reducing the measured current density (I_m) with I_{TE}, I_{DT} and I_{TFE}, represents the leakage component contributed by the sum of I_P and I_{TD}.

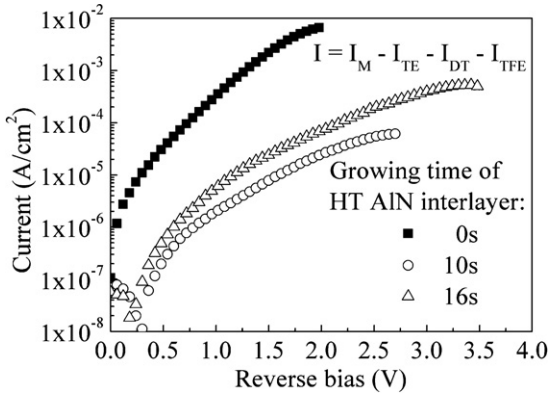

Figure 3. Reverse-biased leakage current density (I_m–I_{TE}–I_{DT}–I_{TFE}) for S2 (dark squares), S4 (open circles) and S6 (open triangles) as a function of reverse bias.

Further study is required to distinguish between I_P and I_{TD}. Zhang *et al* have suggested that the surface depressions and pits were attributed to the termination of TDs with a screw component [14]. In this sense, the leakage current I_P may contain those contributed by TDs (I_{TD}). Figure 3 shows the contribution of I_P and I_{TD} for S2, S4 and S6 in the reverse-bias range. The calculated value is, to some extent, proportional to the effective area of pinholes and clusters of pinholes as shown in figures 2(*a*)–(*c*). Therefore, we believe that the leakage through pinholes and clusters of pinholes make the main contribution to the leakage current in SCs to $Al_{0.25}Ga_{0.75}N$/GaN heterostructures.

Typical DLTS spectra of S2, S4 and S6 are shown in figure 4. *I–V* and *C–V* measurements are performed at first to decide the reverse bias (V_b) used in DLTS measurements. The pinch-off voltages for S2, S4 and S6 are -2.3 V, -3.05 V and -4.2 V, respectively. Accordingly, DLTS spectra for these three samples are taken at the pinch-off region, -1.8 V for S2, -2.7 V for S4 and -3.7 V for S6. The forward-going filling pulse heights (V_f) are all 0.5 V. The low leakage current at V_b (all are less than 5 μA) and low series resistance enable us to get reliable DLTS results. Two deep level electron traps with the activation energies 0.499 eV (called A_1) and 0.924 eV, have been found in the i-GaN epilayer (the DLTS spectrum of S1 is not shown here). Their apparent capture-cross-section are 1.3×10^{-16} cm^2 and 2.5×10^{-13} cm^2, respectively. We believe that A_1 in i-GaN is in the same deep levels as those observed in the GaN epilayer [15, 16]. Fang *et al* have suggested this

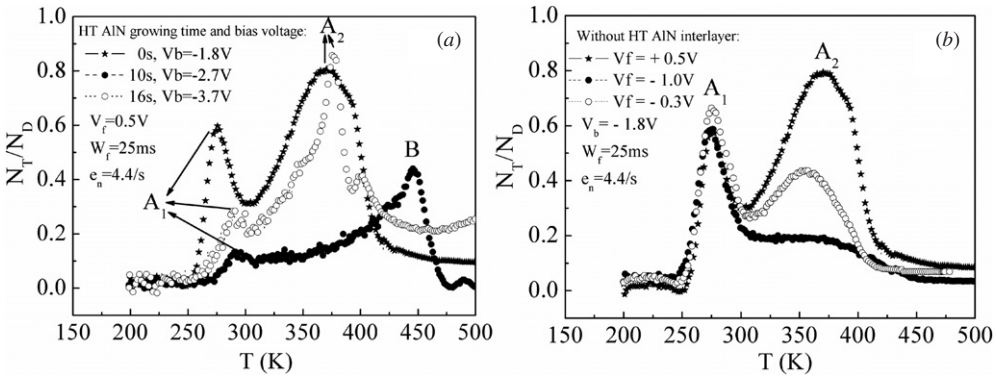

Figure 4. (*a*) DLTS spectra of samples S2 (dark squares), S4 (open circles) and S6 (open triangles) measured at the pinch-off region with the same forward-going filling pulse height V_f. (*b*) DLTS spectra of sample S2 measured at the pinch-off region with three different forward-going filling pulse heights V_f.

trap was a line defect in reactive molecular beam epitaxy GaN [16].

The trap A_1 has been also detected in S2, S4 and S6, as shown in figure 4(*a*), although its density and peak positions are different from each other. Arrhenius analysis indicates that A_1 in these three samples have nearly the same activation energy. The density difference may be caused by the different width of the space-charge region extended in i-GaN, which depends on the applied reverse bias. Anyway, the trap A_1 is confirmed in i-GaN. The important thing is the electron trap A_2 with the activation energy of 0.762 eV and apparent capture cross section of 3.4×10^{-16} cm^2. Its density decreases with increasing growth time of the HT AlN interlayer first, and then changes to decrease after the growth time exceeds 10 s. Such behavior is just as the reverse-biased leakage does. The narrower full-width at half-maximum of S6 in DLTS and the appearance of another peak on the closer right reflect the different surface morphology of AFM between S2 and S6. The electron trap B, with an activation energy of 1.095 eV and an apparent capture cross section of 2.9×10^{-13} cm^2, appears only in S4, need further investigation.

To ascertain the spatial location of the trap A_2, DLTS spectra as a function of V_f (by decreasing V_f from 0.5 to −1.0 V) in S2 is measured. As shown in figure 4(*b*), it is very interesting that the density of trap A1 keeps nearly unchanged, while the density of A_2 decreases rapidly as V_f decreases from 0.5 V to −1.0 V. Both S4 and S6 show the same change tendency. It should be stated out that only traps located in the depth range defined by a pair of pulse bias (V_b and V_f) contribute to the DLTS signal [17]. Considering the large activation energy (0.762 eV) and the obvious difference in density, trap A_2 should lie in the $Al_{0.25}Ga_{0.75}N$ barrier. If A_2 is a trap in i-GaN or an interface state at $Al_{0.25}Ga_{0.75}N$/GaN heterointerface, the curves of two different V_f, 0.5 V and −0.3 V, should have the same shape, in view of the energy band diagram of $Al_xGa_{1-x}N$/GaN heterostructure [18]. The origin of the A_2 trap is under investigation. It may have a relationship with TDs in the $Al_{0.25}Ga_{0.75}N$ barrier [5, 19]. Nevertheless, the similar changing tendency among DLTS, AFM and reverse-biased *I–V* reveal that the leakage via the trap A2 is probably the main leakage current mechanism in Schottky contacts to $Al_{0.25}Ga_{0.75}N$/GaN heterostructures.

4. Conclusions

The leakage current mechanism in SCs to $Al_{0.25}Ga_{0.75}N$/GaN heterostructures with different HT AlN interlayer thickness has been investigated by *I–V*, AFM and DLTS measurements. It is found that the HT AlN interlayer thickness has a significant effect on the leakage current in SCs to $Al_{0.25}Ga_{0.75}N$/GaN heterostructures. The leakage current density decreases to 1.1×10^{-4} A cm^{-2} when the growth time of the AlN interlayer increases from 0 to 10 s, and then changes to increase with increasing growth time. Correspondingly, the heterostructure with the AlN growth time of 10 s has the best surface morphology. HT AlN thickness also influences significantly the density of the electron trap with the activation energy of 0.762 eV in the $Al_{0.25}Ga_{0.75}N$ barrier. It is suggested that the HT AlN interlayer adjusts the microstructure and the defect state density in the $Al_{1-x}Ga_xN$ barrier, and the leakage via these traps makes the main contribution to the leakage current in SCs to $Al_{1-x}Ga_xN$/GaN heterostructures.

Acknowledgments

This work was supported by the National Natural Science Foundation of China (nos10774001, 60736033 and 60628402), National Basic Research Program of China (nos2006CB604908 and 2006CB921607), the Cultivation Fund of the Key Scientific and Technical Innovation Project, Ministry of Education of China (no705002), the Research Fund for the Doctoral Program of Higher Education in China (20060001018) and Beijing Natural Science Foundation (no4062017).

References

[1] Mishra U K, Parikh P P and Wu Y F 2002 *Proc. IEEE* **90** 1022
[2] Karmalkar S, Sathaiya D M and Shur M S 2003 *Appl. Phys. Lett.* **82** 3976
[3] Levinshtein M E, Rumyantsev S L, Gaska R, Wang J W and Shur M S 1998 *Appl. Phys. Lett.* **73** 1089
[4] Hsu L and Walukiewicz W 2001 *J. Appl. Phys.* **89** 1783
[5] Çörekçi S, Öztürk M K, Akaoglu B, Çakmak M and Özcelik S 2007 *J. Appl. Phys.* **101** 123502
[6] Zhang H, Miller E T and Yu E T 2006 *J. Appl. Phys.* **99** 023703

[7] Hasegawa H and Oyama S 2002 *J. Vac. Sci. Technol.* B **20** 1467
[8] Chen C H, Baier S M, Arch D K and Shur M S 1988 *IEEE Trans. Electron Device* **35** 570
[9] Geng L, Ponce F A, Tanaka S, Omiya H and Nakagawa Y 2001 *Phys. Status Solidi* A **188** 803
[10] Lee I H, Kim T G and Park Y 2002 *J. Cryst. Growth* **234** 305
[11] Smorchkova I P, Chen L, Mates T, Shen L, Heikman S, Moran B, Denbaars S P, Speck J S and Mishra U K 2001 *J. Appl. Phys.* **90** 5196
[12] Hsu J W P, Manfra M J, Molnar R J, Heying B and Speck J S 2002 *Appl. Phys. Lett.* **81** 79
[13] Wang M J, Shen B, Xu F J, Wang Y and Xu J 2007 *Appl. Phys.* A **88** 715
[14] Zhang A P, Rowland L B, Kaminsky E B, Tilak V, Grande J C, Teetsov J, Vertiatchikh A and Eastman L F 2003 *J. Electron. Mater.* **32** 388
[15] Götz W, Johnson N M, Amano H and Akasaki I 1994 *Appl. Phys. Lett.* **65** 463
[16] Fang Z Q, Look D C and Polenta L 2002 *J. Phys.: Condens. Matter.* **14** 13061
[17] Lefevre H and Schulz M 1977 *Appl. Phys.* **12** 45
[18] Osvald J 2007 *Appl. Phys.* A **87** 679
[19] Langer J M and Heinrich H 1985 *Phys. Rev. Lett.* **55** 1414